

Susan J. Smith, Steven Brookes-Fazakerley, Louise E. Donnelly, Peter J. Barnes, Mary S. Barnette and Mark A. Giembycz

Am J Physiol Lung Cell Mol Physiol 284:279-289, 2003. First published Oct 4, 2002;
doi:10.1152/ajplung.00170.2002

You might find this additional information useful...

This article cites 44 articles, 15 of which you can access free at:

<http://ajplung.physiology.org/cgi/content/full/284/2/L279#BIBL>

This article has been cited by 4 other HighWire hosted articles:

The Pharmacology of Two Novel Long-Acting Phosphodiesterase 3/4 Inhibitors, RPL554 [9,10-Dimethoxy-2-(2,4,6-trimethylphenylimino)-3-(N-carbamoyl-2-aminoethyl)-3,4,6,7-tetrahydro-2H-pyrimido[6,1-a]isoquinolin-4-one] and RPL565 [6,7-Dihydro-2-(2,6-diisopropylphenoxy)-9,10-dimethoxy-4H-pyrimido[6,1-a]isoquinolin-4-one]

V. Boswell-Smith, D. Spina, A. W. Oxford, M. B. Comer, E. A. Seeds and C. P. Page
J. Pharmacol. Exp. Ther., August 1, 2006; 318 (2): 840-848.

[\[Abstract\]](#) [\[Full Text\]](#) [\[PDF\]](#)

COPD: current therapeutic interventions and future approaches

P. J. Barnes and R. A. Stockley
Eur. Respir. J., June 1, 2005; 25 (6): 1084-1106.

[\[Abstract\]](#) [\[Full Text\]](#) [\[PDF\]](#)

A-Kinase Anchoring Proteins Interact with Phosphodiesterases in T Lymphocyte Cell Lines

A. L. Asirvatham, S. G. Galligan, R. V. Schillace, M. P. Davey, V. Vasta, J. A. Beavo and D. W. Carr

J. Immunol., October 15, 2004; 173 (8): 4806-4814.

[\[Abstract\]](#) [\[Full Text\]](#) [\[PDF\]](#)

Anti-Inflammatory Potential of the Selective Phosphodiesterase 4 Inhibitor N-(3,5-Dichloro-pyrid-4-yl)-[1-(4-fluorobenzyl)-5-hydroxy-indole-3-yl]-glyoxylic Acid Amide (AWD 12-281), in Human Cell Preparations

R. Draheim, U. Egerland and C. Rundfeldt
J. Pharmacol. Exp. Ther., February 1, 2004; 308 (2): 555-563.

[\[Abstract\]](#) [\[Full Text\]](#) [\[PDF\]](#)

Updated information and services including high-resolution figures, can be found at:

<http://ajplung.physiology.org/cgi/content/full/284/2/L279>

Additional material and information about *AJP - Lung Cellular and Molecular Physiology* can be found at:

<http://www.the-aps.org/publications/ajplung>

This information is current as of July 6, 2009 .

Ubiquitous expression of phosphodiesterase 7A in human proinflammatory and immune cells

SUSAN J. SMITH,¹ STEVEN BROOKES-FAZAKERLEY,¹ LOUISE E. DONNELLY,¹
PETER J. BARNES,¹ MARY S. BARNETTE,² AND MARK A. GIEMBYCZ¹

¹Thoracic Medicine, National Heart and Lung Institute, Faculty of Medicine, Imperial College of Science, Technology and Medicine, London SW3 6LY, United Kingdom; and ²Department of Pulmonary Pharmacology, GlaxoSmithKline, King of Prussia, Pennsylvania 19406-0939

Submitted 3 June 2002; accepted in final form 26 September 2002

Smith, Susan J., Steven Brookes-Fazakerley, Louise E. Donnelly, Peter J. Barnes, Mary S. Barnette, and Mark A. Giembycz. Ubiquitous expression of phosphodiesterase 7A in human proinflammatory and immune cells. *Am J Physiol Lung Cell Mol Physiol* 284: L279–L289, 2003. First published October 4, 2002; 10.1152/ajplung.00170.2002.—We have determined the expression of phosphodiesterase (PDE) 7A1 and PDE7A2 in human cells that have been implicated in the pathogenesis of chronic obstructive pulmonary disease and asthma. Messenger RNA transcripts were detected by RT-PCR in T lymphocytes, monocytes, neutrophils, airway and vascular smooth muscle cells, lung fibroblasts, epithelial cells, and cardiac myocytes. Human epithelial, T cell, eosinophil, and lung fibroblast cell lines were also positive for PDE7A1 and PDE7A2 mRNA transcripts. By Western immunoblot analyses the amount of PDE7A1 was greatest in T cell lines, peripheral blood T lymphocytes, epithelial cell lines, airway and vascular smooth muscle cells, lung fibroblasts, and eosinophils but was not detected in neutrophils. In contrast, PDE7A2 protein, which was identified in human cardiac myocytes, was not found in any of the other cell types investigated. Immunofocal analyses showed that PDE7A was expressed in neutrophils and alveolar macrophages. As the expression of PDE7A mirrors the distribution of PDE4 we speculate that this enzyme could be a target for novel anti-inflammatory drugs.

inflammation; lung

CYCLIC NUCLEOTIDE PHOSPHODIESTERASES (PDEs) comprise a large family of enzymes that metabolize the ubiquitous second messengers adenosine 3',5'-cyclic monophosphate (cAMP) and guanosine 3',5'-cyclic monophosphate (cGMP) to their respective inactive 5'-monophosphates. Currently, 11 different PDE families have been described that differ in tissue distribution and molecular and physicochemical characteristics including primary sequence, substrate specificity, inhibitor sensitivity, and cofactor requirements (40). It is now appreciated that multiple genes within each family encode PDEs with additional diversity arising from mRNA splicing and differential promoter usage (7, 22). The cAMP-specific PDE4 isoenzyme family is one of the

most extensively studied PDEs. Enzymes within this family are found in most proinflammatory and immune cells, where they are important regulators of cAMP metabolism. Moreover, PDE4 inhibitors abrogate inflammation in animal models of respiratory diseases, which has led to the view that PDE4 may represent a target amenable to therapeutic intervention with small molecule inhibitors. Although the use of PDE4 inhibitors for the treatment of airway inflammation is based on a conceptually robust hypothesis (14, 15, 40, 41), dose-limiting side effects, of which nausea and vomiting are the most common and worrisome, have hampered their clinical development (14, 40). Moreover, these adverse effects represent an extension of the pharmacology of these compounds (8), and improving the therapeutic ratio of PDE4 inhibitors has proved a major challenge that is still on-going.

Several strategies have been considered to dissociate the beneficial and detrimental effects of PDE4 inhibitors (14, 40) with some degree of success (15). However, compounds with an optimal pharmacophore have not yet been described. An alternative approach is to target other cAMP PDE families that are expressed in proinflammatory and immune cells in the hope that therapeutic activity can be divorced from side effects. One such candidate is PDE7, which was first isolated at the gene level in 1993 from a human glioblastoma cDNA library and expressed in a cAMP-deficient strain of the yeast *Saccharomyces cerevisiae* (29). PDE7A encodes a cAMP-specific PDE that is insensitive to cGMP and inhibitors of PDE3 and PDE4 and has an amino acid sequence distinct from other cAMP PDEs (29). In humans (13, 20, 35) and mice (13, 20), two genes (*PDE7A* and *PDE7B*) have been identified that encode PDE7. With respect to PDE7A, three isoenzymes (PDE7A1, PDE7A2, and PDE7A3) can theoretically be derived from the same gene by alternative mRNA splicing. PDE7A2 is generated from a 5'-splice variant and, therefore, differs from PDE7A1 in its NH₂-terminal domain (4, 18). In mice and humans, PDE7A2 mRNA is expressed abundantly in skeletal muscle, heart, and

Address for reprint requests and other correspondence: M. A. Giembycz, Thoracic Medicine, National Heart and Lung Institute, Faculty of Medicine, Imperial College of Science, Technology and Medicine, London SW3 6LY, UK (E-mail: m.giembycz@ic.ac.uk).

The costs of publication of this article were defrayed in part by the payment of page charges. The article must therefore be hereby marked "advertisement" in accordance with 18 U.S.C. Section 1734 solely to indicate this fact.

kidney, whereas the testis, lung, and immune system (thymus, spleen, lymph node, blood leukocytes) are rich sources of *HSPDE7A1*, where HS refers to *Homo sapiens* (4, 18, 42). In activated, but not naïve, human T lymphocytes a third, COOH-terminal splice variant, PDE7A3, was found recently (17). In contrast, PDE7B exists as a single isoenzyme in humans with ~70% sequence similarity to, and distinct kinetic properties from, PDE7A (13, 20, 35), whereas in the rat three splice variants of PDE7B can be derived (34). PDE7B is expressed predominantly in the brain and in a number of other tissues including liver, heart, thyroid glands, and skeletal muscle (13, 20, 35). It is not expressed in blood leukocytes (13).

Compared with PDE4, little is known of the expression of PDE7A in cells that have been implicated in the pathogenesis of asthma and chronic obstructive pulmonary disease (COPD). It has been reported that PDE7A mRNA is present in primary epithelial cells (11, 44) and human peripheral blood T lymphocytes (16) and B lymphocytes (12). Protein and message for PDE7A1 and PDE7A3 are also expressed in several T cell lines (4) and human peripheral blood T lymphocytes (17, 25). PDE7A1 protein has also been recently found in human splenic B lymphocytes (24). Moreover, functional studies, using antisense oligonucleotides, indicate a role for PDE7A in T cell proliferation and interleukin (IL)-2 production (25), suggesting that inhibition of this enzyme may, indeed, represent a potential target for novel anti-inflammatory drugs. Indeed, CD4⁺ and CD8⁺ T lymphocytes are elevated in the airways of patients with asthma and COPD, respectively, where they may play a major role in orchestrating mucosal inflammation (23, 33). Several preliminary studies and anecdotal reports at scientific meetings and in review articles have indicated that PDE7 mRNA is present in other proinflammatory and immune cells, but these observations have not been confirmed.

As a first step to understanding the functional role of PDE7A, we have performed a systematic study, at the mRNA and protein level, to determine the expression of PDE7A1 and PDE7A2 in human cells that have been implicated in the pathogenesis of airway inflammatory diseases including COPD and asthma.

MATERIALS AND METHODS

Patients providing blood samples and those who underwent sputum induction or bronchoalveolar lavage (BAL) gave written informed consent. The Ethics Committee of the Royal Brompton Hospital approved this study.

Purification of leukocytes. Blood was collected from normal healthy individuals by antecubital venepuncture into acid citrate dextrose (160 mM disodium citrate, 11 mM glucose, pH 7.4), and leukocytes were purified as described below.

T lymphocytes and monocytes. T lymphocytes (CD4⁺ and CD8⁺) and monocytes were purified from the peripheral blood mononuclear cell (PBMC) fraction, which was obtained from density gradient centrifugation of anticoagulated blood on Ficoll-Hypaque (Amersham Pharmacia Biotech, Little Chalfont, UK). Blood was diluted 1:1 with Hanks' balanced salt solution (HBSS), layered onto Ficoll-Hypaque (1.077 g/ml), and centrifuged (400 g, 20 min) at room temperature.

PBMCs were harvested from the plasma/Ficoll-Hypaque interface, washed twice in HBSS, and further purified by negative immunoselection using the magnetic cell sorting system (Miltenyi Biotech, Bisley, UK) according to the manufacturer's instructions to obtain highly purified T lymphocyte subsets and monocytes. The cocktail used to isolate the CD4⁺ T lymphocytes included antibodies against CD8, CD11b, CD16, CD19, CD36, and CD56. A similar cocktail was used to prepare the CD8⁺ T lymphocytes, with the exception that the antihuman CD8 antibody was replaced with an antihuman CD4 antibody.

Eosinophils. Eosinophils were isolated from peripheral blood with slight modifications to an established method (19). Briefly, anticoagulated blood was mixed with Elohaes (Fresenius Kabi, Runcorn, UK) and incubated at room temperature for 60 min to sediment the erythrocytes. The leukocyte-rich supernatant was layered onto Ficoll-Hypaque and centrifuged (400 g, 20 min) at room temperature. Granulocytes were harvested from below the Ficoll-Hypaque layer and washed twice in HBSS, and residual erythrocytes were removed by ice-cold hypotonic lysis. The granulocytes were incubated with microbeads coupled to antihuman CD16, according to the manufacturer's instructions (Miltenyi Biotech), and eosinophils were enriched by negative selection.

Neutrophils. Neutrophils were prepared by incubating anticoagulated peripheral blood for 60 min with Elohaes to sediment the erythrocytes. The leukocyte-rich supernatant was removed, and the cells were washed with HBSS, layered over a discontinuous (63% vol/vol and 73% vol/vol) Percoll gradient (Amersham Pharmacia Biotech), and centrifuged (450 g, 30 min, at 18°C). Neutrophils were isolated from the 63%/73% Percoll interface and washed twice with HBSS.

Culture of smooth muscle cells, cell lines, and cardiac myocytes. Human airway (ASM) and vascular smooth muscle (VSM) cells were cultured from tracheal rings and lung-derived pulmonary artery, respectively (21, 43). Cells were routinely used between passages 4 and 9. Jurkat and HUT-78 T cells were cultured at 10⁶ ml⁻¹ in RPMI 1640 (Sigma Aldrich) supplemented with 10% (vol/vol) heat-inactivated fetal bovine serum (FBS) and 2 mM L-glutamine (Sigma Aldrich) and passaged every 2–3 days. Human fibroblasts, obtained from extracts of lung parenchyma, and the MRC-5 fetal lung fibroblast cell line were cultured in Dulbecco's modified Eagle's medium supplemented with 10% (vol/vol) FBS and 2 mM L-glutamine. Cells were used between passages 5 and 9. A549 and U-937 cells were both cultured in RPMI 1640 supplemented with 10% (vol/vol) FBS and 2 mM L-glutamine, whereas AML14.3D10 cells were cultured in the same medium supplemented with 1 mM sodium pyruvate, 50 μM β-mercaptoethanol, and 50 μg/ml gentamicin (Invitrogen Life Technologies, Paisley, UK). BEAS-2B and 16HBE14o⁻ were cultured in keratinocyte medium containing epithelial growth factor and bovine pituitary extract (Invitrogen Life Technologies), and minimal essential medium containing 10% FBS, 2 mM L-glutamine, and 1% (vol/vol) nonessential amino acids (Sigma Aldrich), respectively. Myocardial biopsies were obtained and treated as previously described (3).

Sputum induction and processing. Sputum was induced in normal volunteers by 3 × 5 min inhalations of nebulized hypertonic saline (3.5% wt/vol). The procedure was stopped if the forced expiratory volume in one second dropped by >10% in response to saline or by >20% at any other time during the induction procedure. The sputum samples were weighed, and dithiothreitol (Sigma Aldrich), dissolved in 0.1% wt/vol phosphate-buffered saline (PBS), was added in a ratio of 4 ml to 1 g of sputum and incubated at room temperature for 15 min

on a rolling mixer. PBS was added to the sputum and then filtered through 48- μ m nylon gauze. The filtrate was centrifuged (250 g, 10 min), and the cells were washed twice with PBS. The sputum cells were finally resuspended at a concentration of 10^6 /ml, and 100 μ l of cell suspension were used to prepare cytopspins. Thus cells were centrifuged (450 rpm, 3 min) onto poly-L-lysine-coated slides (Merck Eurolabs, Luttermouth, UK) using a Shandon II cytocentrifuge (Shandon, Runcorn, UK), air dried for 1 h at room temperature, wrapped in foil, and stored desiccated at -70°C .

BAL. Subjects were premedicated intramuscularly with atropine (0.5 mg) and diazepam (10 mg) and orally with dihydrocodeine (10 mg). The nose and throat were anesthetized topically with 10% (wt/vol) lidocaine. Bronchoscopy was performed with a flexible fiberoptic bronchoscope (Pentax FB-18P; Asahi Optical, Tokyo, Japan). Two 60-ml aliquots of warmed, sterile saline solution were introduced, and returned fluid was collected by gentle machine suction, followed by a further 60-ml aliquot. Aspirated fluid was collected into a sterile siliconized glass bottle and cooled gradually to 4°C . The fluid was filtered through 100- μ m nylon gauze, and the filtrate was centrifuged (250 g, 10 min). Cells were washed twice with RPMI 1640 supplemented with 10% (vol/vol) FBS and 2 mM L-glutamine and cultured for 4 h at 37°C in six-well plates at a concentration of 2×10^6 /ml. Nonadherent cells were removed and cytocentrifuged onto poly-L-lysine-coated slides as described above.

Tissue macrophages. Lung tissue was obtained from patients undergoing surgical resection for carcinoma. The tissue was lavaged with RPMI supplemented with 10% (vol/vol) FBS, 2 mM L-glutamine, 100 units/ml penicillin, 100 μ g/ml streptomycin, and 2.5 μ g/ml amphotericin. The cells were washed twice with medium, and macrophages were either purified on a discontinuous Percoll gradient or cytopspins of the mixed cell preparation were prepared as described in *Sputum induction and processing*.

Semiquantitative RT-PCR. Total RNA was extracted from cells using RNeasy kits according to the manufacturer's instructions (Qiagen, Crawley, UK), and all preparations were treated with RNase-free DNase (Qiagen) to remove genomic DNA. RNA was quantified spectrophotometrically, and 0.5 μ g was reverse transcribed in a total volume of 20 μ l in the presence of 7.2 units avian myeloblastosis virus RT (Promega, Southampton, UK), 30 units RNase inhibitor (Promega), and 0.2 μ g random hexanucleotides. RT-generated cDNAs encoding *HSPDE7A1* and *HSPDE7A2* were amplified using the specific primers shown in Table 1. The forward primers for PDE7A1 and PDE7A2 were described by Miro et al. (30), and the reverse primers were described by Han et al. (18). To confirm the integrity of RNA and equal loading of samples and to gain an estimate of the level of PDE7 expression, we also performed RT-PCR of the GAPDH gene, using primers described by Maier et al. (27) (Table 1).

PCR amplification was conducted in a reaction volume of 25 μ l using a Hybaid Omnigene thermal cycler (Hybaid, Teddington, UK) and 0.5 units of *Taq* polymerase (Bioline, London, UK). The number of cycles chosen for the PCR reactions was determined empirically from cDNA pooled from a mixture of peripheral blood leukocytes and primary cells. PCR products were analyzed on 1% (wt/vol) agarose gels, stained with ethidium bromide, and visualized under ultraviolet light. Quantification of the PCR products was carried out with Gelworks ID Intermediate software (Ultraviolet Products, Cambridge, UK). To confirm identity with published sequences, we sequenced PDE7A amplification products using a BigDye terminator cycle sequencing kit (ABI-Prism, Warrington Cheshire, UK) according to manufacturer's instructions, and the samples were run on a 310 Genetic Analyser (ABI-Prism).

Western immunoblot analysis. Cells were lysed in ice-cold buffer [10 mM Tris·HCl, pH 7.4, 150 mM NaCl, 1 mM EDTA, 1% (vol/vol) Nonidet P-40, 0.25% (wt/vol) sodium deoxycholate, 0.1% (wt/vol) SDS, and 0.25% (vol/vol) Triton X-100] supplemented with 0.1 mg/ml phenylmethylsulfonyl fluoride, 10 μ g/ml leupeptin, 25 μ g/ml aprotinin, 10 μ g/ml pepstatin, 10 μ g/ml sodium orthovanadate, 0.1 mg/ml sodium fluoride, and 0.2 mg/ml sodium pyrophosphate (all Sigma Aldrich) and were centrifuged (12,000 g, 10 min) to remove insoluble material. The lysates were diluted (5:1) in sample buffer [62.5 mM Tris, 10% (vol/vol) glycerol, 1% (wt/vol) SDS, 1% (vol/vol) β -mercaptoethanol, and 0.01% (wt/vol) bromophenol blue, pH 6.8] and boiled for 5 min. Denatured proteins (20 μ g) were subsequently separated by electrophoresis on 8% (wt/vol) or 4–12% (wt/vol) gradient SDS polyacrylamide vertical gels and transferred to Hybond ECL membranes (Amersham) in 50 mM Tris base, pH 8.3, 192 mM glycine, and 20% (vol/vol) methanol. Nonspecific binding sites were blocked by immersing the membranes in nonfat milk [5% (wt/vol) in Tris-buffered saline (TBS)-Tween 20] for 1 h at room temperature. PDE7A expression was detected by either a rabbit or a goat anti-PDE7A antibody, which is specific for a 15- and 21-amino acid sequence at the COOH-terminal end of the protein, respectively (Santa Cruz Biotechnology, Santa Cruz, CA). Primary labeling was performed at room temperature with 2 μ g/ml of the goat anti-PDE7A or 1 μ g/ml of the rabbit anti-PDE7A in nonfat milk (5% wt/vol in TBS-Tween 20) for 1 h at room temperature. After 3×5 min washes in TBS-Tween 20, the membranes were incubated for 60 min with a peroxidase-conjugated sheep anti-goat Ig antibody or peroxidase-conjugated goat anti-rabbit antibody (both Dako). The membranes were washed again (5×5 min), and the antibody-labeled proteins were visualized by enhanced chemiluminescence (Amersham).

To ascertain the specificity of the anti-PDE7A antibody, the antibody was preadsorbed with the peptide used as the immunogen, incubated overnight at 4°C with gentle agita-

Table 1. Primers used in RT-PCR experiments

Gene Product	GenBank Accession No.	Deoxynucleotide Sequence	Cycle Number	Coordinates of PCR Products in Human cDNA Sequence	Product Size, bp	Annealing Temperature, $^\circ\text{C}$
PDE7A1	L12052	Forward: 5'-GGCAGGGCGGGCGTATTCA-3' Reverse: 5'-CATGGCCTGAGTAACATCCGC-3'	30	32–50 722–702	690	60
PDE7A2	U67932	Forward: 5'-ATTGATCTGGTGTCTGGCCTTGG-3' Reverse: 5'-as for PDE7A1	32	168–190 750–730	582	61
GAPDH	BC0016001	Forward: 5'-CCACCATGGCAAATTCATGGCA-3' Reverse: 5'-TCTAGACGGCAGGTCAGGTCCACC-3'	27	206–229 803–780	598	58

PDE, phosphodiesterase.

tion and then diluted to the desired working concentration. The membranes were stripped and then reprobed with the "blocked" antibody as described above.

Immunocytochemistry. PDE7A expression was analyzed using the rabbit antibody described above for Western blotting. Cytospins were allowed to equilibrate to room temperature and then fixed in 4% (wt/vol) paraformaldehyde in PBS (pH 7.4) for 10 min. After 3×5 min washes in PBS, the slides were incubated with either 1 μ g/ml of the rabbit anti-PDE7A antibody or a rabbit Ig antibody control (Dako, Ely, UK) in PBS (pH 7.4) containing 10% (vol/vol) normal human serum (NHS) for 1 h at room temperature. The slides were washed (3×5 min in PBS), and a biotin-conjugated goat anti-rabbit Ig was used in conjunction with an avidin-biotin-alkaline phosphatase detection system (Vector Laboratories, Peterborough, UK). The reaction was visualized using fast red in the presence of levamisole (Vector Laboratories), and the cells were subsequently counterstained with hematoxylin (Merck Eurolabs) and mounted using glycerol (Dako).

Triple-label immunofocal laser microscopy. Mixed cell populations (from sputum and BAL fluid samples and lung parenchyma) were first labeled with the rabbit anti-PDE7A antibody and avidin-biotin alkaline phosphatase detection kit with fast red substrate (Vector Laboratories) as described above. Mouse monoclonal antibodies specific for either neutrophil elastase (clone NP57) or CD68 (clone EMB11) (both Dako) were subsequently used to identify neutrophils and macrophages, respectively. The monoclonal antibodies were incubated for 1 h in PBS/10% (vol/vol) NHS at room temperature. A Bodipy-conjugated goat anti-mouse IgG antibody (Molecular Probes, Leiden, Netherlands) was incubated for 1 h in PBS/10% (vol/vol) NHS at room temperature and used to detect the phenotypic markers in cells from sputum, BAL fluid, and lung parenchyma. The slides were washed and subsequently incubated with diaminidino phenylindole (DAPI) at 10 μ M (Sigma Aldrich) in HBSS for 3 min, washed again, and mounted using PBS/50% (vol/vol) glycerol. Cells (0.7 μ m sections) were analyzed under a Leica TCS 4D confocal microscope (Leica Microsystems, Milton Keynes, UK) equipped with argon, krypton, and ultraviolet lasers. Confocal images were acquired at $\times 40$ magnification.

RESULTS

The expression of PDE7A in human proinflammatory and immune cells was determined by RT-PCR, Western blotting, immunocytochemistry (ICC), and immunofocal laser microscopy. This multidisciplinary approach allowed a systematic analysis of many cells to be performed, including alveolar macrophages and airway neutrophils, that are implicated in the pathogenesis of airway inflammatory diseases such as asthma and COPD.

Expression of HSPDE7A1 and HSPDE7A2 mRNA. Messenger RNA transcripts for *HSPDE7A1* and *HSPDE7A2* were detected by RT-PCR using primers that recognize unique sequences in the human *PDE7A* gene (29). Figure 1 shows ethidium bromide-stained agarose gels of representative experiments. In five independent determinations using cells from different donors, PCR products corresponding to the predicted sizes of *HSPDE7A1* (690 bp) and *HSPDE7A2* (582 bp) were detected in CD4⁺ T lymphocytes, CD8⁺ T lymphocytes, neutrophils, monocytes, ASM cells, VSM cells, and lung fibroblasts. The abundance of these

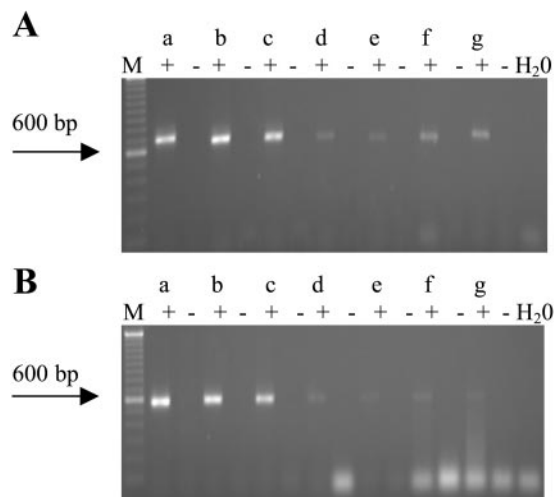


Fig. 1. Qualitative RT-PCR analysis of phosphodiesterase (PDE) 7 mRNA isoforms in highly purified human peripheral blood leukocytes, smooth muscle cells, and lung fibroblasts. Representative ethidium bromide-stained agarose gels of sample cDNA processed in the absence (-) and presence (+) of RT (to control for genomic contamination), respectively, are shown. RT-PCR product sizes for *HSPDE7A1* (A) and *HSPDE7A2* (B) were 690 bp (30 cycles) and 582 bp (32 cycles), respectively, where HS refers to *Homo sapiens*. Lanes H₂O and M in each gel are negative control (sterile water) and molecular weight markers (0.25 μ g of 100-bp ladder; Invitrogen, Life Technologies), respectively. The figure shows CD4⁺ T lymphocytes (a), CD8⁺ T lymphocytes (b), monocytes (c), neutrophils (d), airway smooth muscle (ASM) cells (e), vascular smooth (VSM) cells (f) and lung fibroblasts (g). The gels are representative of 5 independent experiments. See MATERIALS AND METHODS for further details.

PDE7A splice variants did not vary significantly between donors when related to the housekeeping gene GAPDH (Fig. 2). Human T lymphocytic (HUT-78, Jurkat), epithelial (16-HBE14, BEAS-2B), monocytic (U-937), eosinophilic (AML14.3D10) (2), and fetal lung fibroblast (MRC-5) cell lines also expressed both splice variants of PDE7A (Table 2) with PDE7A1 representing the primary transcript. The identity of the PCR products was confirmed by sequencing (data not shown).

In all cell types studied, mRNA for PDE7A1 was generally more abundant than PDE7A2. Indeed, 30 and 32 cycles of amplification were required to produce similar amounts of PDE7A1 and PDE7A2 PCR product, respectively (Fig. 1). In contrast, the PDE7A2 transcript predominated in human ventricular cardiac myocytes. Moreover, of the primary cells studied, PDE7A1 and PDE7A2 PCR products, generated from 0.5 μ g of total RNA, were more abundantly expressed in lymphocytes and monocytes than in neutrophils, lung fibroblasts, and ASM and VSM cells (Fig. 1).

Expression of PDE7A1 and PDE7A2 protein by Western immunoblot analysis. In cells that could be obtained in reasonable numbers and of high purity, PDE7A isoform expression was determined by Western blotting using a goat polyclonal antibody raised against a 21-amino acid sequence in the COOH-terminal portion of PDE7A, which is common to both PDE7A1 and PDE7A2 (it does not recognize PDE7A3). In these experiments, the T cell line HUT-78 and

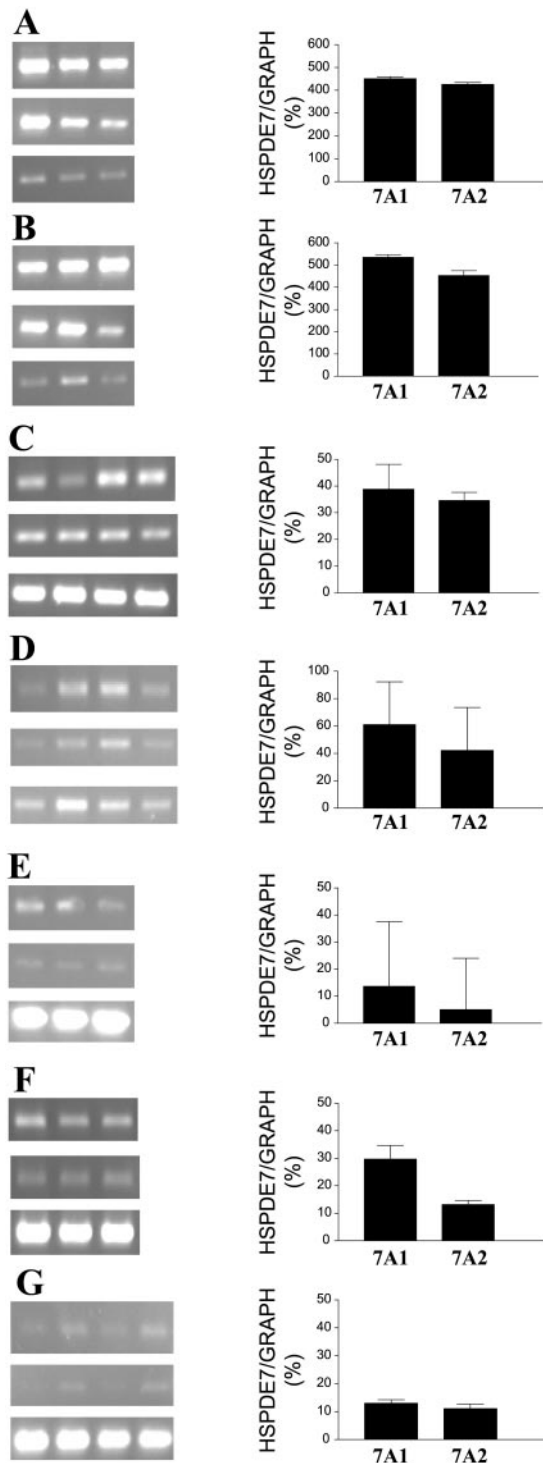


Fig. 2. Semiquantitative RT-PCR analysis of PDE7 mRNA isoforms in highly purified human peripheral blood leukocytes, smooth muscle cells, and lung fibroblasts relative to the expression of GAPDH. The figure shows ethidium bromide-stained agarose gels of cDNA from CD4⁺ T lymphocytes (A), CD8⁺ T lymphocytes (B), monocytes (C), neutrophils (D), ASM cells (E), VSM cells (F), and lung fibroblasts (G). Data are representative of 3 or 4 determinations and are expressed relative to GAPDH. See MATERIALS AND METHODS for further details.

human ventricular cardiac myocytes were used as positive controls for PDE7A1 (4) and PDE7A2 (18), respectively. As shown in Fig. 3A, the anti-PDE7A antibody detected a protein from CD4⁺ and CD8⁺ T lymphocytes that migrated as a 57-kDa band on SDS polyacrylamide gels. This immunoreactive protein was identical in size to PDE7A1 expressed by HUT-78 cells and of a molecular mass consistent with human recombinant PDE7A1 expressed in Sf9 insect cells (4). PDE7A1 was most highly expressed in T lymphocyte subsets and, normally, human ASM cells (but see below) with a relatively lower level of expression in monocytes and eosinophils (Fig. 4). PDE7A1 was not detected in neutrophils by Western blotting (Fig. 4). A consistent finding of this study was the variable expression of PDE7A1 in human cultured ASM cells (see Fig. 4), which might relate to passage number, intrinsic differences in expression between donors, or medication.

Several cell lines of the immune system also expressed a 57-kDa PDE7A variant that had the characteristics of PDE7A1 and included BEAS-2B and 16HBE140⁻ epithelial cells and the Jurkat T cell line, as well as MRC-5 fibroblasts (Fig. 4) and eosinophil-like AML14.3D10 cells (not shown). U-937 monocytes were also positive for HSPDE7A1, but expression was relatively low. In some experiments, the goat anti-PDE7A antibody labeled a doublet in BEAS-2B and 16HBE140⁻ cell lysates that migrated at 57 and ~59 kDa (Fig. 4B). To determine whether the higher-molecular-weight species could be a phosphorylated form of PDE7A1, we pretreated cells with okadaic acid (50 nM, 30 min), an inhibitor of type 1 and type 2A protein phosphatases, before Western blotting. However, the intensity of the higher-molecular-weight species was not increased by okadaic acid, suggesting that it is unlikely to be phospho-PDE7A1. This conclusion is supported by the failure of another PDE7A antibody (raised in rabbits) to detect the ~59-kDa peptide (Fig. 4C).

The specificity of the rabbit anti-PDE7A antibody, which was used for ICC and confocal microscopy (see below), is shown in Fig. 4C. For all samples except the neutrophil (which was PDE7A⁻), the major immunoreactive peptide migrated at 57 kDa on SDS polyacrylamide gels. However, proteins migrating at ~200 kDa (e.g., HUT-78, CD4⁺-T cells, BEAS-2B, human cultured ASM) and 10 kDa (e.g., macrophages) were sometimes labeled by the antibody, although expression was always weak relative to PDE7A.

PDE7A2 protein was not detected in any of the immune or proinflammatory cells studied despite the unambiguous identification of PCR products corresponding to *HSPDE7A2* mRNA (Figs. 1 and 2). However, initial studies detected a 50-kDa PDE7A-immunoreactive protein in CD4⁺ and CD8⁺ T lymphocytes (Fig. 3A). When the same samples were resolved using 4–12% (wt/vol) gradient gels, the bands migrated at a different mobility to the PDE7A2 in cardiac myocytes (Fig. 3B) and are, therefore, unlikely to represent the same protein. In contrast, the anti-PDE7A antibody

Table 2. Expression of mRNA and protein for HSPDE7A in human proinflammatory and immune cells

Cell Type	mRNA		Protein	
	HSPDE7A1	HSPDE7A2	HSPDE7A1	HSPDE7A2
<i>Human Primary Cells</i>				
CD4 ⁺ T lymphocyte	+	+	+	-
CD8 ⁺ T lymphocyte	+	+	+	-
B lymphocyte (12, 24)		+	+	ND
Neutrophil	+	+		+
Alveolar macrophage	+	+		+
Monocyte	+	+	+	-
Eosinophil	ND	ND	+	-
Bronchial epithelial cell (11, 44)		+		ND
Lung mast cell (32)		+		-
Lung basophil (32)		+		-
Airway smooth muscle cell	+	+	+	-
Vascular smooth muscle cell	+	+	+	-
Vascular endothelial cell (30)	+	+	ND	ND
Cardiac myocyte	+	+	-	+
<i>Human Cell Lines</i>				
HUT-78 (T cell)	+	+	+	-
Jurkat (T cell)	+	+	+	-
16-HBE14 (epithelial cell)	+	+	+	-
NCIH292 (36) (epithelial cell)		+	ND	ND
BEAS-2B (epithelial cell)	+	+	+	-
U-937 (monocyte)	+	+	+	-
MRC-5 (fibroblast)	+	+	+	-
AML14.3D10 (eosinophil)	+	+	+	-
Jiyoye (4) (B cell)	+	ND	-	ND

+, Enzyme detected; -, enzyme not detected; ND, not determined; *, isoenzyme not determined; HSPDE, *Homo sapiens* phosphodiesterase. Numbers in parentheses refer to references.

labeled a protein from ventricular cardiac myocytes that migrated as a 50-kDa peptide on SDS polyacrylamide gels, which is in agreement with the reported molecular mass of PDE7A2 expressed in the yeast plasmid ADHSM7 (18).

Detection of HSPDE7A by ICC and immunofocal laser microscopy. ICC was used to investigate PDE7A expression in purified cells, and immunofocal laser microscopy was used to determine PDE7A expression in proinflammatory and immune cells in sputum and BAL fluid and in cells where PDE7A expression was not detected by either ICC or Western blotting. In the ICC experiments, PDE7A⁺ cells stained red. Cell nuclei stained a dark blue, and cell cytoplasm stained a lighter blue with hematoxylin. As shown in Fig. 5, HUT-78 T cells (Fig. 5B), CD4⁺ (Fig. 5D) and CD8⁺ (Fig. 5F) T lymphocytes, as well as monocytes (Fig. 5H), ASM cells (Fig. 5J), VSM cells (Fig. 5L), and lung fibroblasts (Fig. 5N) stained positive for PDE7A, whereas negligible and nonspecific staining was detected with the rabbit Ig control antibody (Fig. 5, A, C, E, G, I, K, and M). Neutrophils were also PDE7A⁺, but expression was weak (Fig. 6B). The presence of PDE7A in human eosinophils could not be established due to nonspecific reactivity of one or more components of the avidin-biotin alkaline phosphatase system with these cells.

To verify the expression of PDE7A in neutrophils, we employed immunofocal laser microscopy. Evaluation of the fluorescence emission of the fast red substrate after excitation at 568 nm demonstrated that

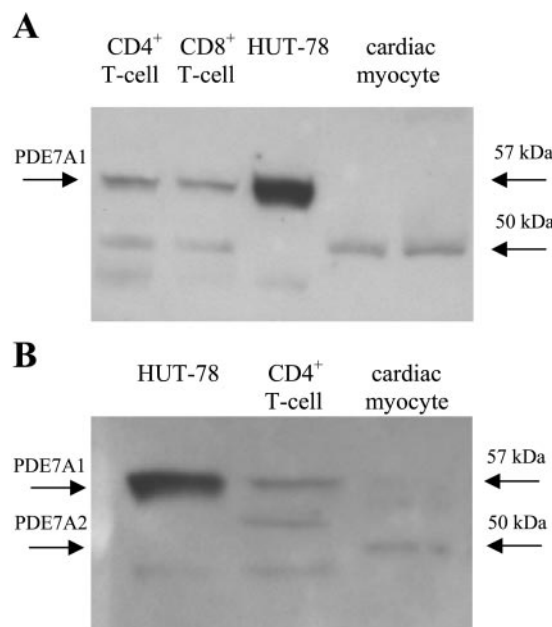


Fig. 3. Western blot analysis of PDE7A expression in human peripheral blood CD4⁺ and CD8⁺ T lymphocytes, HUT-78 T cells, and cardiac myocytes. Highly purified cells were lysed, insoluble proteins were removed, and 20 μ g of soluble extract were denatured and subjected to electrophoresis on 8% (wt/vol) SDS polyacrylamide gels (A) or 4–12% (wt/vol) gradient gels (B). Proteins were transferred to nitrocellulose and probed with anti-PDE7A antibody at 2 μ g/ml. The nitrocellulose was subsequently incubated with a peroxidase-conjugated sheep anti-goat antibody, and labeled proteins were detected by enhanced chemiluminescence. These data are representative of 4 identical experiments. See MATERIALS AND METHODS for further details.

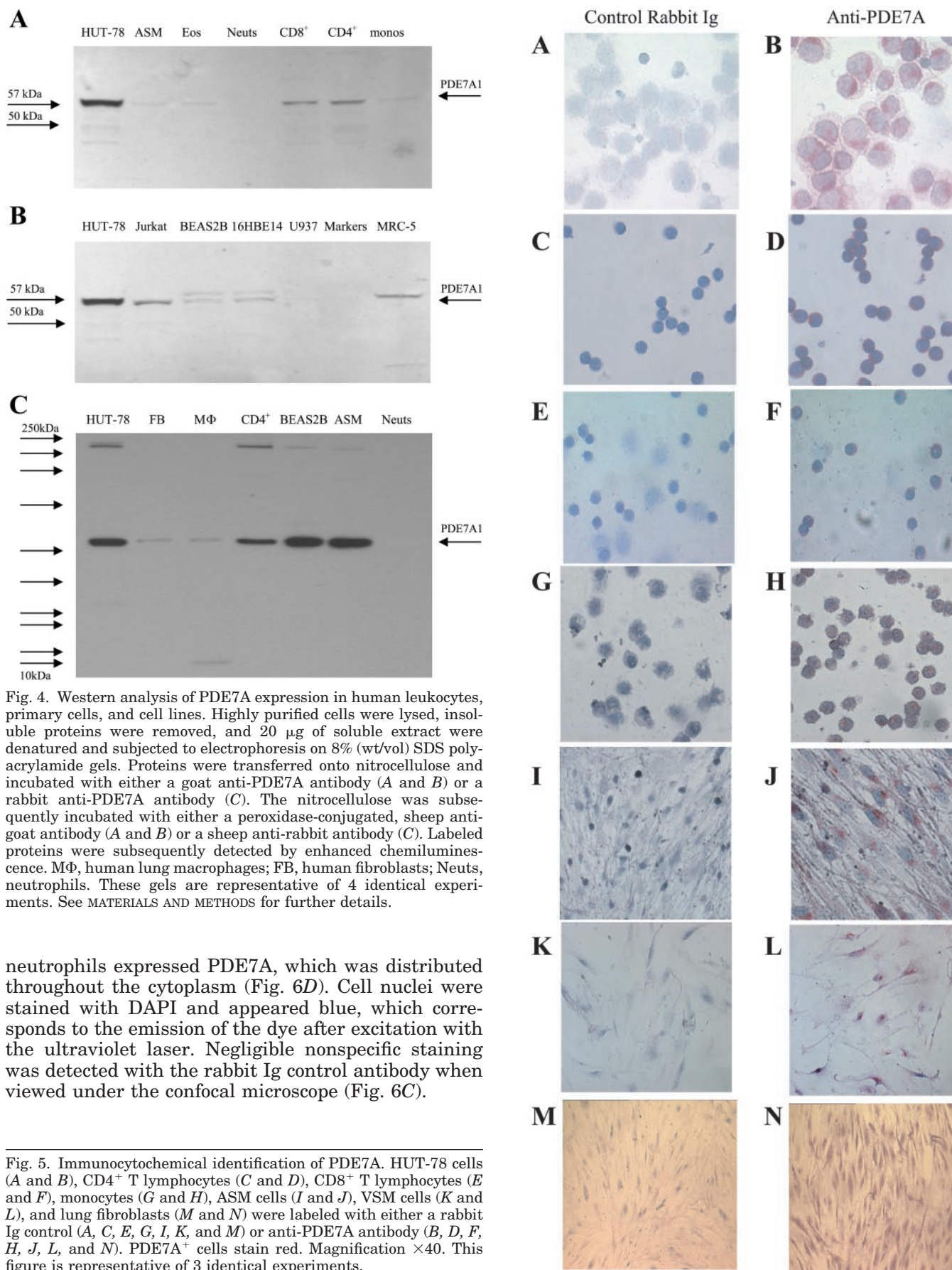


Fig. 4. Western analysis of PDE7A expression in human leukocytes, primary cells, and cell lines. Highly purified cells were lysed, insoluble proteins were removed, and 20 μ g of soluble extract were denatured and subjected to electrophoresis on 8% (wt/vol) SDS polyacrylamide gels. Proteins were transferred onto nitrocellulose and incubated with either a goat anti-PDE7A antibody (A and B) or a rabbit anti-PDE7A antibody (C). The nitrocellulose was subsequently incubated with either a peroxidase-conjugated, sheep anti-goat antibody (A and B) or a sheep anti-rabbit antibody (C). Labeled proteins were subsequently detected by enhanced chemiluminescence. M Φ , human lung macrophages; FB, human fibroblasts; Neuts, neutrophils. These gels are representative of 4 identical experiments. See MATERIALS AND METHODS for further details.

neutrophils expressed PDE7A, which was distributed throughout the cytoplasm (Fig. 6D). Cell nuclei were stained with DAPI and appeared blue, which corresponds to the emission of the dye after excitation with the ultraviolet laser. Negligible nonspecific staining was detected with the rabbit Ig control antibody when viewed under the confocal microscope (Fig. 6C).

Fig. 5. Immunocytochemical identification of PDE7A. HUT-78 cells (A and B), CD4⁺ T lymphocytes (C and D), CD8⁺ T lymphocytes (E and F), monocytes (G and H), ASM cells (I and J), VSM cells (K and L), and lung fibroblasts (M and N) were labeled with either a rabbit Ig control (A, C, E, G, I, K, and M) or anti-PDE7A antibody (B, D, F, H, J, L, and N). PDE7A⁺ cells stain red. Magnification \times 40. This figure is representative of 3 identical experiments.

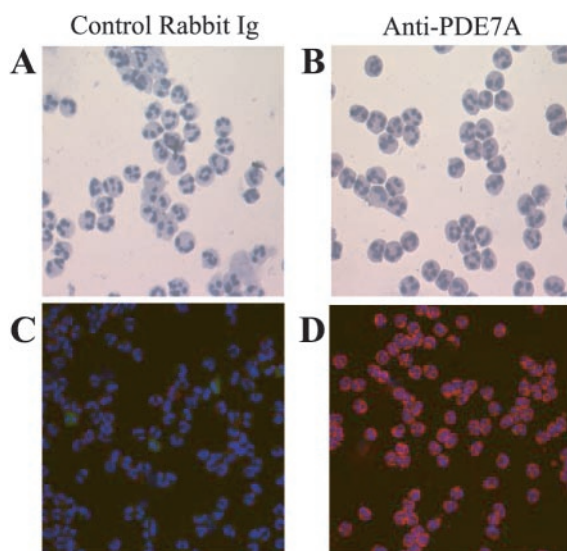


Fig. 6. Immunocytochemical and immunofluorescence identification of PDE7A in human peripheral blood neutrophils. Highly purified peripheral blood neutrophils were stained with a rabbit Ig control (A and C) or anti-PDE7A antibody (B and D). The neutrophils were visualized by either light microscopy (A and B) or confocal fluorescence microscopy (C and D) where PDE7A⁺ cells stain red. Blue staining indicates nuclei. This figure is representative of 5 experiments.

Triple-label immunofluorescence analysis was performed on cells present in induced sputum and BAL fluid of normal individuals and from lung parenchyma. Cells that expressed elastase or CD68, which are specific phenotypic markers of neutrophils and macrophages, respectively, appear green after excitation of the Bodipy label at 488 nm. The red and blue coloration in the confocal images represents PDE7A⁺ and nuclei, respectively. With the use of this method, sputum-derived neutrophils (Fig. 7B) and macrophages (Fig. 7D) were PDE7A⁺. There was no significant staining of either neutrophils (Fig. 7A) or macrophages (Fig. 7C) in the sputum (or BAL fluid and lung parenchyma, data not shown) when the control rabbit Ig was used.

DISCUSSION

This paper describes the distribution of PDE7A across human proinflammatory and immune cells that are implicated in the pathogenesis of asthma and COPD. Consistent with the results of previous investigations (14, 16, 17, 25, 37), PDE7A was detected unequivocally in human CD4⁺ and CD8⁺ T lymphocytes and the T cell lines HUT-78 and Jurkat (4). However, mRNA transcripts and protein for PDE7A were not restricted to T cells. Indeed, this enzyme was distributed across almost all cells studied (Table 2), suggesting that PDE7A may be involved in regulating many cAMP-dependent responses.

PDE7A mRNA expression. In all cells studied, PDE7A1 and PDE7A2 mRNA was detected, although, with semiquantitative RT-PCR, the latter transcript was approximately fourfold less abundant. These re-

sults contrast with the distribution of PDE7A mRNAs in other human peripheral tissues such as skeletal muscle, where the PDE7A2 transcript predominates (18), although they agree with expression data in human fetal tissues (18). PDE7A2 mRNA encodes an enzyme with a novel 20-amino acid hydrophobic NH₂ terminus, which is thought to be responsible for tethering the enzyme to cell membranes. In contrast, PDE7A1, which lacks this hydrophobic domain, can be either cytosolic or particulate (18). Thus it seems highly likely that PDE7A splice variants regulate different functional responses and are, themselves, subject to distinct modes of regulation. Moreover, the predominance of PDE7A1 mRNA is consistent with the cytosolic distribution of PDE7A1 protein in proinflammatory and immune cells.

PDE7A protein expression. In cells that could be obtained in high numbers and purity, Western blotting was used to determine the expression of PDE7A protein using an antibody that recognizes PDE7A1 and PDE7A2. In these experiments, HUT-78 T cells (4) and human cardiac myocytes (29) were used as positive controls for PDE7A1 and PDE7A2, respectively. In contrast to a previous report (25), freshly isolated peripheral blood-derived T lymphocytes expressed a PDE7A variant that comigrated, with a HUT-78 cell extract, as a 57-kDa protein on SDS polyacrylamide gels indicative of PDE7A1. A likely reason for this discrepancy may be attributed to the method of purifi-

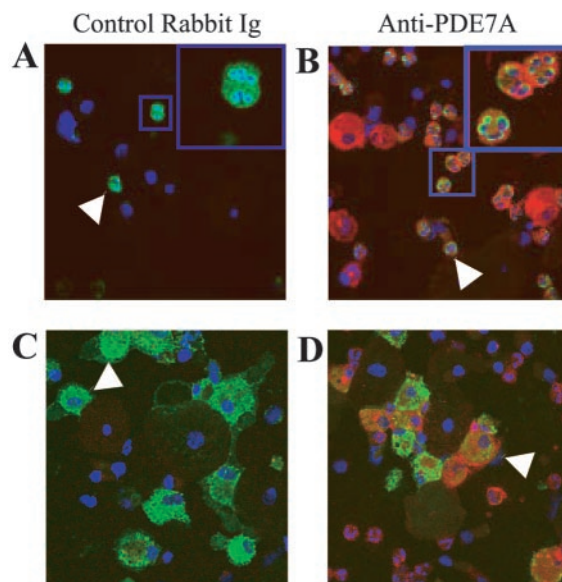


Fig. 7. Immunofluorescence identification of PDE7A in cells in human sputum. Cell preparations were stained with a rabbit Ig control antibody (A and C) or an anti-PDE7A antibody (B and D). Neutrophils and macrophages were labeled with an antielastase antibody (A and B) and an anti-CD68 antibody (C and D) respectively. PDE7A⁺ cells stain red. Phenotypic markers for cells stain green. Blue staining indicates nuclei. White arrowhead in A and C: an elastase⁺ neutrophil and CD68⁺ macrophage, respectively. White arrows in B and D: a PDE7A⁺ elastase⁺ neutrophil and PDE7A⁺ CD68⁺ macrophage, respectively. Enlarged images of the elastase⁺ neutrophils and PDE7A⁺ elastase⁺ neutrophils are also shown in A and B, respectively. This figure is representative of 6 experiments.

cation (25). In the present study, T lymphocytes were isolated from other leukocytes by negative immunoselection by a mixture of antibodies against CD11b, CD16, CD19, CD36, CD56, and either CD4 (for CD8⁺ cells) or CD8 (for CD4⁺ cells). However, in the experiments where PDE7A1 was not detected, antibodies against CD25 and HLA-DR were also used (17), which will remove all activated and proliferating T cells. Collectively, these data suggest that naïve T lymphocytes express significantly less PDE7A1 than circulating blood T lymphocytes, many of which will be undergoing cell division.

PDE7A1 was also detected in monocytes and ASM and VSM cells, although on a protein basis expression was lower than that found in T lymphocytes. A number of cell lines (Table 2) were PDE7A1⁺ with the highest expression found in epithelial cell lines and the lowest in U-937 monocytic cells. In none of the immune or proinflammatory cells examined did either of the anti-PDE7A antibodies detect the 50-kDa PDE7A2 variant (cf. cardiac myocytes) despite the unambiguous identification of PCR products corresponding to *PDE7A2* mRNA at an abundance only approximately fourfold lower than that of PDE7A1 (see above). Similar results have been reported in murine skeletal muscle and the Jiyoye human B cell line where mRNA but little, if any, protein for PDE7A1 was detected (4). These findings are not peculiar to PDE7A. In human mononuclear cells and T lymphocytes, several of the *HSPDE4D* splice variants are expressed at the mRNA level only (31, 38). The reason(s) for these discrepancies is unclear. It is plausible that the amount of PDE7A2 protein expressed in leukocytes is below the detection limit of the techniques applied in the present study. This interpretation would be consistent with the relatively low abundance of PDE7A2 mRNA transcripts relative to PDE7A1. Instability of the active enzyme and/or a low translation rate of PDE7A2 mRNA are other possibilities, which could suggest that the stability and translation of PDE7A protein are highly regulated processes in these cells.

Western blotting failed to detect PDE7A in neutrophils. To establish whether this enzyme was, indeed, absent from these cells or merely below the detection limit of this method, ICC and immunofocal laser microscopy were employed. These techniques were also used to determine the expression of PDE7A in cells present in sputum and BAL fluid with emphasis on alveolar macrophages and neutrophils. Using these more sensitive methods, we found PDE7A in peripheral blood and airway neutrophils, as well as alveolar macrophages. PDE7A was also detected by ICC in these cells from patients with asthma and COPD. However, the lack of bands on Western blots suggests that the concentration of PDE7A in these cells is lower than that found in the other cell types examined. Although ICC and immunofocal laser microscopy could not distinguish the PDE7A splice variants, much of the staining was cytosolic, indicating that PDE7A1 may be the most abundant isoform expressed.

Until relatively recently, cAMP PDE activity in Ca²⁺-free cell and tissue lysates that persists in the presence of a maximally effective concentration of a PDE2, PDE3, and PDE4 inhibitor has been attributed to PDE7 (11). Indeed, this approach has led investigators to propose that PDE7 activity is present in a number of cells, including T lymphocytes (16, 39), BEAS-2B cells, and human airway epithelial cells (11). However, identification of PDE7 by this method is no longer valid, as additional cAMP PDE families also resistant to PDE2, PDE3, and PDE4 inhibitors have been described, including PDE8 (10), PDE10 (26), and PDE11 (9). Thus until selective inhibitors become available, the contribution of PDE7 to the regulation of cAMP hydrolysis in cells and tissues cannot easily be determined.

Therapeutic potential of PDE7 inhibitors. An intriguing finding of these studies was that the distribution of PDE7A1 mirrors the expression pattern of PDE4. Thus PDE7A1 has been identified in cells thought to be central to the pathogenesis of asthma and COPD, including CD4⁺ and CD8⁺ T lymphocytes, monocytes, neutrophils, and alveolar macrophages together with ASM and VSM. Although PDE7A inhibitors have become available (1, 5, 24, 28), they are not selective for *in vitro* or *in vivo* use. However, it is tempting to speculate that they may suppress a myriad of proinflammatory responses similar to those effected by PDE4 inhibitors such as rolipram. Indeed, stimulation of human naïve peripheral blood-derived T lymphocytes with anti-CD3 and anti-CD28 antibodies has been shown to promote IL-2 production and proliferation (25). These effects were associated with induction of PDE7A1 and prevented by antisense oligonucleotides directed against PDE7A (17). Thus PDE7A could represent a target for novel anti-inflammatory drugs, particularly for use in airway inflammatory diseases. This is an important consideration as the clinical efficacy of current PDE4 inhibitors (e.g., cilomilast) for the treatment of asthma and COPD, although demonstrable (6, 15), is compromised by dose-limiting side effects (14, 15, 40, 41).

In conclusion, in this study we have found by Western analysis, ICC, and immunofocal microscopy that PDE7A is distributed ubiquitously across a variety of cells that have been implicated in the inflammation that characterizes asthma and COPD. As PDE7A inhibitors become available, it is certain that a major research effort will begin to determine the functional role of PDE7A in these cells and whether such compounds have anti-inflammatory activity similar to rolipram without the associated gastrointestinal, cardiovascular, and central nervous system side effects.

The authors thank Ben Booy for technical assistance with the confocal microscope and Dr. Louise Pulleyn for sequencing the RT-PCR products. The authors acknowledge Gina Jones, Lorraine Matthews, and Suzanne Traves for the culture of the epithelial cell lines and the U-937 cells; Deborah Clarke, Dr. Hema Patel, and Dr. Maria Sukkar for the culture of the human ASM cells; and Dr. Steven Wort for culture of the human VSM cells. We thank the staff of the Clinical Studies Unit, Royal Brompton Hospital, London, for the collection

and processing of induced sputum samples; Dr. Borja Cosio for providing BAL fluid cells; and Dr. Virginia Owen for providing human cardiac tissue for Western analysis. The authors also thank Cassandra Paul and Michael Baumann at Wright State University for the AML14.3D10 cell line and Prof. Gruenert, University of Vermont, for the 16HBE14o⁻ bronchial epithelial cell line.

S. J. Smith and M. A. Giembycz are supported by GlaxoSmith-Kline, Stevenage, UK.

REFERENCES

- Barnes MJ, Cooper N, Davenport RJ, Dyke HJ, Galleway FP, Galvin FC, L Gowers L, Haughan AF, Lowe C, Meissner JW, Montana JG, Morgan T, Picken CL, and Watson RJ. Synthesis and structure-activity relationships of guanine analogues as phosphodiesterase 7 (PDE7) inhibitors. *Bioorg Med Chem Lett* 11: 1081–1083, 2001.
- Baumann MA and Paul CC. The AML14 and AML14.3D10 cell lines: a long-overdue model for the study of eosinophils and more. *Stem Cells* 16: 16–24, 1998.
- Birks EJ, Yacoub MH, Burton PS, Owen V, Pomerance A, O'Halloran A, Banner NR, Khaghani A, and Latif N. Activation of apoptotic and inflammatory pathways in dysfunctional donor hearts. *Transplantation* 70: 1498–1506, 2000.
- Bloom TJ and Beavo JA. Identification and tissue-specific expression of PDE7 phosphodiesterase splice variants. *Proc Natl Acad Sci USA* 93: 14188–14192, 1996.
- Castro A, Abasolo MI, Gil C, Segarra V, and Martinez A. CoMFA of benzyl derivatives of 2,1,3-benzo and benzothieno[3,2-alpha]thiadiazine 2,2-dioxides: clues for the design of phosphodiesterase 7 inhibitors. *Eur J Med Chem* 36: 333–338, 2001.
- Compton CH, Gubb J, Nieman R, Edelson J, Amit O, Bakst A, Ayres JG, Creemers JP, Schultze-Werninghaus G, Brambilla C, and Barnes NC. Cilomilast, a selective phosphodiesterase-4 inhibitor for treatment of patients with chronic obstructive pulmonary disease: a randomised, dose-ranging study. *Lancet* 358: 265–270, 2001.
- Conti M and Jin SL. The molecular biology of cyclic nucleotide phosphodiesterases. *Prog Nucleic Acid Res Mol Biol* 63: 1–38, 1999.
- Duplantier AJ, Biggers MS, Chambers RJ, Cheng JB, Cooper K, Damon DB, Egger JF, Kraus KG, Marfat A, Masamune H, Pillar JS, Shirley JT, Umland JP, and Watson JW. Biarylcarboxylic acids and -amides: inhibition of phosphodiesterase type IV versus [3H]rolipram binding activity and their relationship to emetic behavior in the ferret. *J Med Chem* 39: 120–125, 1996.
- Fawcett L, Baxendale R, Stacey P, McGrouther C, Harrow I, Soderling S, Hetman J, Beavo JA, and Phillips SC. Molecular cloning and characterization of a distinct human phosphodiesterase gene family: PDE11A. *Proc Natl Acad Sci USA* 97: 3702–3707, 2000.
- Fisher DA, Smith JF, Pillar JS, St. Denis SH, and Cheng JB. Isolation and characterization of PDE8A, a novel human cAMP-specific phosphodiesterase. *Biochem Biophys Res Commun* 246: 570–577, 1998.
- Fuhrmann M, Jahn HU, Seybold J, Neurohr C, Barnes PJ, Hippenstiel S, Kraemer HJ, and Suttorp N. Identification and function of cyclic nucleotide phosphodiesterase isoenzymes in airway epithelial cells. *Am J Respir Cell Mol Biol* 20: 292–302, 1999.
- Gantner F, Gotz C, Gekeler V, Schudt C, Wendel A, and Hatzelmann A. Phosphodiesterase profile of human B lymphocytes from normal and atopic donors and the effects of PDE inhibition on B cell proliferation. *Br J Pharmacol* 123: 1031–1038, 1998.
- Gardner CN, Robas D, Cawkill D, and Fidock M. Cloning and characterization of the human and mouse PDE7B, a novel cAMP-specific cyclic nucleotide phosphodiesterase. *Biochem Biophys Res Commun* 272: 186–192, 2000.
- Giembycz MA. Phosphodiesterase 4 inhibitors and the treatment of asthma: where are we now and where do we go from here? *Drugs* 59: 193–212, 2000.
- Giembycz MA. Cilomilast: a second generation phosphodiesterase 4 inhibitor for asthma and chronic obstructive pulmonary disease. *Expert Opin Investig Drugs* 10: 1361–1379, 2001.
- Giembycz MA, Corrigan CJ, Seybold J, Newton R, and Barnes PJ. Identification of cyclic AMP phosphodiesterases 3, 4 and 7 in human CD4⁺ and CD8⁺ T-lymphocytes: role in regulating proliferation and the biosynthesis of interleukin-2. *Br J Pharmacol* 118: 1945–1958, 1996.
- Glavas NA, Ostenson C, Schaefer JB, Vasta V, and Beavo JA. T cell activation up-regulates cyclic nucleotide phosphodiesterases 8A1 and 7A3. *Proc Natl Acad Sci USA* 98: 6319–6324, 2001.
- Han P, Zhu X, and Michaeli T. Alternative splicing of the high affinity cAMP-specific phosphodiesterase (PDE7A) mRNA in human skeletal muscle and heart. *J Biol Chem* 272: 16152–16157, 1997.
- Hansel TT, Pound JD, Pilling D, Kitas GD, Salmon M, Gentle TA, Lee SS, and Thompson RA. Purification of human blood eosinophils by negative selection using immunomagnetic beads. *J Immunol Methods* 122: 97–103, 1989.
- Hetman JM, Soderling SH, Glavas NA, and Beavo JA. Cloning and characterization of PDE7B, a cAMP-specific phosphodiesterase. *Proc Natl Acad Sci USA* 97: 472–476, 2000.
- Hirst SJ, Barnes PJ, and Twort CH. Quantifying proliferation of cultured human and rabbit airway smooth muscle cells in response to serum and platelet-derived growth factor. *Am J Respir Cell Mol Biol* 7: 574–581, 1992.
- Houslay MD. PDE4 cAMP-specific phosphodiesterases. *Prog Nucleic Acid Res Mol Biol* 69: 249–315, 2001.
- Jeffery PK. Lymphocytes, chronic bronchitis and chronic obstructive pulmonary disease. *Novartis Found Symp* 234: 149–161, 2001.
- Lee R, Wolda S, Moon E, Esselstyn J, Hertel C, and Lerner A. PDE7A is expressed in human B-lymphocytes and is up-regulated by elevation of intracellular cAMP. *Cell Signal* 14: 277–284, 2002.
- Li L, Yee C, and Beavo JA. CD3- and CD28-dependent induction of PDE7 required for T cell activation. *Science* 283: 848–851, 1999.
- Loughney K, Snyder PB, Uher L, Rosman GJ, Ferguson K, and Florio VA. Isolation and characterization of PDE10A, a novel human 3', 5'-cyclic nucleotide phosphodiesterase. *Gene* 234: 109–117, 1999.
- Maier JA, Hla T, and Maciag T. Cyclooxygenase is an immediate-early gene induced by interleukin-1 in human endothelial cells. *J Biol Chem* 265: 10805–10808, 1990.
- Martinez A, Castro A, Gil C, Miralpeix M, Segarra V, Domenech T, Beleta J, Palacios JM, Ryder H, Miro X, Bonet C, Casacuberta JM, Azorin F, Pina B, and Puigdomenech P. Benzyl derivatives of 2,1,3-benzo- and benzothieno[3,2-a]thiadiazine 2,2-dioxides: first phosphodiesterase 7 inhibitors. *J Med Chem* 43: 683–689, 2000.
- Michaeli T, Bloom TJ, Martins T, Loughney K, Ferguson K, Riggs M, Rodgers L, Beavo JA, and Wigler M. Isolation and characterization of a previously undetected human cAMP phosphodiesterase by complementation of cAMP phosphodiesterase-deficient *Saccharomyces cerevisiae*. *J Biol Chem* 268: 12925–12932, 1993.
- Miro X, Casacuberta JM, Gutierrez-Lopez MD, de Landazuri MO, and Puigdomenech P. Phosphodiesterases 4D and 7A splice variants in the response of HUVEC cells to TNF-alpha. *Biochem Biophys Res Commun* 274: 415–421, 2000.
- Nemoz G, Zhang R, Sette C, and Conti M. Identification of cyclic AMP-phosphodiesterase variants from the PDE4D gene expressed in human peripheral mononuclear cells. *FEBS Lett* 384: 97–102, 1996.
- Peachell PT, Weston MC, and Drummer J. Characterisation of phosphodiesterases in human lung mast cells and basophils (Abstract). *Br J Pharmacol* 134: 67P, 2001.
- Renauld JC. New insights into the role of cytokines in asthma. *J Clin Pathol* 54: 577–589, 2001.

34. **Sasaki T, Kotera J, and Omori K.** Novel alternative splice variants of rat phosphodiesterase 7B showing unique tissue-specific expression and phosphorylation. *Biochem J* 361: 211–220, 2002.
35. **Sasaki T, Kotera J, Yuasa K, and Omori K.** Identification of human PDE7B, a cAMP-specific phosphodiesterase. *Biochem Biophys Res Commun* 271: 575–583, 2000.
36. **Seamons R, Hinzpeter A, MacKenzie C, MacKenzie S, Houslay M, and van Heeke G.** Expression profile of Phosphodiesterases 4, 3 and 7 in resting and activated epithelial cells (Abstract). *Br J Pharmacol* 135: 8P, 2002.
37. **Secchiero P, Zella D, Curreli S, Mirandola P, Capitani S, Gallo RC, and Zauli G.** Pivotal role of cyclic nucleoside phosphodiesterase 4 in Tat-mediated CD4+ T cell hyperactivation and HIV type 1 replication. *Proc Natl Acad Sci USA* 97: 14620–14625, 2000.
38. **Seybold J, Newton R, Wright L, Finney PA, Suttorp N, Barnes PJ, Adcock IM, and Giembycz MA.** Induction of phosphodiesterases 3B, 4A4, 4D1, 4D2, and 4D3 in Jurkat T-cells and in human peripheral blood T-lymphocytes by 8-bromo-cAMP and Gs-coupled receptor agonists. Potential role in beta2-adrenoreceptor desensitization. *J Biol Chem* 273: 20575–20588, 1998.
39. **Tenor H, Staniciu L, Schudt C, Hatzelmann A, Wendel A, Djukanovic R, Church MK, and Shute JK.** Cyclic nucleotide phosphodiesterases from purified human CD4+ and CD8+ T lymphocytes. *Clin Exp Allergy* 25: 616–624, 1995.
40. **Torphy TJ.** Phosphodiesterase isozymes: molecular targets for novel anti-asthma agents. *Am J Respir Crit Care Med* 157: 351–370, 1998.
41. **Torphy TJ, Barnette MS, Underwood DC, Griswold DE, Christensen SB, Murdoch RD, Nieman RB, and Compton CH.** Ariflo (SB 207499), a second generation phosphodiesterase 4 inhibitor for the treatment of asthma and COPD: from concept to clinic. *Pulm Pharmacol Ther* 12: 131–135, 1999.
42. **Wang PP, Wu R, Egan W, and Billah MM.** Cloning, characterization, and tissue distribution of mouse phosphodiesterase 7A1. *Biochem Biophys Res Commun* 276: 1271–1277, 2000.
43. **Wort SJ, Woods M, Warner TD, Evans TW, and Mitchell JA.** Endogenously released endothelin-1 from human pulmonary artery smooth muscle promotes cellular proliferation: relevance to pathogenesis of pulmonary hypertension and vascular remodeling. *Am J Respir Cell Mol Biol* 25: 104–110, 2001.
44. **Wright LC, Seybold J, Robichaud A, Adcock IM, and Barnes PJ.** Phosphodiesterase expression in human epithelial cells. *Am J Physiol Lung Cell Mol Physiol* 275: L694–L700, 1998.

